Chapter 4

Synchronization System Model

The synchronization receiver function is to investigate the symbol timing start and estimate the carrier frequency offset which is due to the misalignments between the transmitter and the receiver oscillators and the phase noise and investigate sector and cell search for the LTE downlink by estimating the cell-ID in order to establish a successful connection with the best possible eNB .At the same time, the cell-ID is required for extracting the reference signals from proper sub-carrier positions, and performs the channel estimation procedure using these reference signals according to [1].

The received signal at the eNB is considered to be

$$y(n) = \{s(n) * h(n)\}e^{j2\pi n\epsilon/N} + r(n) \quad (15)$$

$$s(n) = \sum_{k=0}^{N-1} S(k)e^{j2\pi kn/N} \quad (16)$$

where s(n) is the OFDM transmitted signal ,S(k) is the mapped data on the sub-carriers, h(n) is the impulse response of the channel which impacts with the transmitted signal, r(n) is the additive white Gaussian noise (AWGN) and the effect of the frequency offset appears in $e^{j2\pi n\epsilon/N}$, where ϵ is the frequency offset as a fraction of the sub-carrier spacing.

We will focus in our simulations on the LTE channel models which are Extended Pedestrian A model (EPA), Extended Vehicular A model (EVA) and Extended Typical Urban model (ETU) as shown in [6].

In the receiver the symbol timing start is unknown (the accurate frame start) and also as shown in (15) the signal suffers from carrier frequency offset, so our main target here to retrieve the OFDM symbol start(2).

Here we will introduce some of the previous efforts in the timing synchronization and cell search.

(2) Eliminating frequency offset effect is not in our target in our proposed method.

4.1. Cyclic Prefix Based Method [4]

Here the authors introduced the cyclic prefix based method which is used in [4] using ML estimation [5] to get the symbol timing and the fractional part of the carrier frequency. This has been performed in time domain before the FFT receiver, as after the synchronization Process is finished the received data is transformed on the down-link shared channel into frequency domain to decode the received data.

According to [4], the log-likelihood function for the symbol timing start (θ) and the fractional part of the carrier frequency offset ϵ_F is

$$\Lambda(\theta, \epsilon_F) = 2|\gamma(\theta)| \cos\{2\pi\epsilon_F + \angle\gamma(\theta)\} - \rho\epsilon(\theta) \quad (17)$$

where

$$\gamma(n) = \sum_{k=n}^{n+L-1} r(k)r^*(k+N) \quad (18)$$

and

$$\epsilon(n) = \sum_{k=n}^{n+L-1} |r(k)|^2 + |r(k+N)|^2 \quad (19)$$

where L denotes the CP length, measured in time samples, ρ is the magnitude of the correlation coefficient between $r(k)$and $r(k+N)$ and can be calculated as shown in [4], $\angle$ denotes the argument of a complex number.
The maximum likelihood (ML) of θ and ϵ_F which maximizes (17) is

$$\hat{\epsilon}_{F,ML} = -\frac{1}{2\pi}\angle\gamma(\hat{\theta}_{ML}) \quad (20)$$

$$\hat{\theta}_{ML} = \arg\max_{\theta}\{2|\gamma(\theta)| - \rho\epsilon(\theta)\} \quad (21)$$

The computation of $\gamma(n)$ is a low complexity operation as it can be implemented by following recursive formula

$$\gamma(n+1) = \gamma(n) + r(n+L)r^*(n+L+N) - r(n)r^*(n+N) \quad (22)$$

while $\epsilon(n)$ can be computed in the same way.

4.2. Improved Cell Search and Initial Synchronization Using Almost Half- Complexity (AHC) and Central Self-Correlation (CSC) Detectors [17].

In [17] the authors propose two improved PSS detectors, i.e., Almost Half-Complexity (AHC) and Central Self-Correlation (CSC) detectors, by exploiting the central-symmetric property of ZC sequences.

The AHC detector has exactly the same detection accuracy as that of the conventional detector but with 50% complexity being saved and the proposed CSC detector can further reduce its complexity to 50% that of the AHC detector, however, at a cost of a slight accurate degradation.

In [17] the primary synchronization sequences are represented as

$$\mathbf{z}_M = [\mathrm{ZC}_M^{63}(0), \cdots, \mathrm{ZC}_M^{63}(30), 0, \mathrm{ZC}_M^{63}(32), \cdots, \mathrm{ZC}_M^{63}(62)]^T \quad (23)$$

As mentioned before, ZC sequences with different roots have a low cross correlation among them and enable high PSS identification capability. The channel represented by using $h_{k,m}(z)$ to represent the discrete-time impulse response of the zth tap channel between the mth eNodeB and the kth UE, the related channel response vector can be represented as

$$h_{k,m} = \left[h_{k,m}(0), h_{k,m}(1), \ldots., h_{k,m}(L_{max} - 1)\right]^T \quad (24)$$

L_{max} represents the maximum channel length.

The authors defined x_m which is an N × 1 vector as $x_m = \left[0_{N-62/2}, z_M, 0_{N-64/2}\right]^T$ to represent the primary sequence vector transmitted by the mth eNodeB, where N is the system's IDFT length.

According to [17], the received baseband primary sequence vector in the kth UE, with the Mth eNodeB acting as its serving eNodeB, is given by

$$y_k = E_{k,m} F H_{k,m} x_m + \sum_{z \in \tau_m} E_{k,z} F H_{k,z} x_z + w_k \quad (25)$$

where $E_{k,l}(n) = diag\{1, e^{j2\pi\epsilon_{k,l}/N}, \ldots, e^{j2\pi\epsilon_{k,l}(N-1)/N}\}$, with $\epsilon_{k,l}$representing the normalized frequency offset (frequency offset normalized to a subcarrier spacing of OFDM symbols) between the k^{th} UE and the l^{th} eNodeB. τ_l represents the set of interfering eNodeBs of the lth eNodeB. Note that the ZC sequence roots of the objective and interfering eNodeBs may be identical or not. W_k is a vector of additive white Gaussian noise.

In (26) The non-coherent detection (maximizing the cross-correlation function between the transmitted and received ZC sequences) is presented, as θ represents the discrete-time index of the first received sample and $s_M = \mathrm{F}\left[0_{\mathrm{N}-62/2}, \mathrm{z}_{\mathrm{M}}, 0_{\mathrm{N}-64/2}\right]^{\mathrm{T}}$. The ZC sequence can be identified by the UE as

$$\{\widehat{M}, \widehat{\theta}\} = argmax_{M,\theta}\left\{\left|s_M\left(y_k^{\theta}\right)^H\right|^2\right\}$$
$$= argmax_{M,\theta}\left\{\left|s_M[0]y_k^*[\theta] + s_M[N/2]y_k^*[\theta + N/2] + \Omega_{k,\theta}\right|^2\right\} \quad (26)$$

where

$$y_k^{(\theta)} = [y_k[\theta], y_k[\theta+1], \ldots, y_k[\theta+N-1]]^T$$

$$\Omega_{k,\theta} = \sum_{n=1}^{\frac{N}{2}-1} s_M[n]y_k^*[\theta+n] + \sum_{n=\frac{N}{2}+1}^{N-1} s_M[n]y_k^*[\theta+n] \quad (27)$$

4.2.1. Almost Half-Complexity (AHC)

To reduce the cell search complexity, the almost half complexity detector is applied. The odd-length ZC sequences and their IDFT transforms are always central symmetric, regardless of what the *M* values are. From [17], the central-symmetric character still holds in s_M so,

$$s_M[i] = s_M[N-i] \quad (28)$$

Based on this central symmetric property, $\Omega_{k,\theta}$ can be simplified as

$$\Omega_{k,\theta} = \sum_{n=1}^{\frac{N}{2}-1} s_M[n]y_k^*[\theta+n] + \sum_{n=\frac{N}{2}+1}^{N-1} s_M[n]y_k^*[\theta+n]$$
$$= \sum_{n=1}^{\frac{N}{2}-1} s_M[n]y_k^*[\theta+n] + \sum_{n=1}^{N/2-1} s_M[n]y_k^*[\theta+N-n]$$
$$= \sum_{n=1}^{\frac{N}{2}-1} s_M[n](y_k[\theta+n] + y_k[\theta+N-n])^* \quad (29)$$

Evidently, the central-symmetric property in s_M considerably reduces the computational complexity .In the original method, it requires a total of N complex conjugate multiplication operations for each M. However, the last equation reduces the number of complex conjugate multiplication operations to (N/2 + 1).

4.2.2. Central Self-Correlation (CSC) Detectors

Although AHC reduces the computational complexity of primary sequence acquisition considerably, the complexity in each iteration is still too high, because the sequence root *M* should be identified for each θ. Although primary sequence is transmitted very infrequently (once per 5 ms period), the UE still needs to perform the detection aforementioned every time even if it is actually receiving a data symbol. This kind of operation really has a very low efficiency in terms of either power consumption or cell-search speed. Thanks to the central-symmetric property of ZC sequences as well as their IDFT transforms, and also because this central-symmetric property always holds regardless of the exact *M* values, the PSS acquisition speed can be further simplified by exploiting ZC sequences' central self-correlation property. Once a UE detects the central-symmetric pattern in the received vector, it means a primary synchronization sequence is detected (without knowing the exact *M* value yet).

In [17], the authors defined a timing metric of y_k as

$$Z^c(\theta) = \left| \sum_{n=1}^{\frac{N}{2}-1} \frac{y_k[\theta + N - n].\, y_k^*[\theta + n]}{|y_k[\theta + N - n].\, y_k^*[\theta + n]|} \right|^2 \tag{30}$$

The primary synchronization sequence can be identified at the UE by detecting the locally maximal $Z^c(\theta)$ value, and after a primary sequence is successfully detected, the UE will then identify the *M* value of the detected primary sequence.

4.3. Time Synchronization Depending on Partial Correlation Timing Synchronization Algorithm [18].

In [18] new symbol timing synchronization algorithm which combined with differential correlation and the method for accumulation of the received signals is proposed and this method compete the frequency offset effect on the results. In order to reduce the computational load of the proposed algorithm, the correlation between the sum of three groups of local PSS sequence and the received signals was employed.

The new technique was explained in [18] as followed.

4.3.1 Partial Correlation Timing Synchronization

As mentioned before the received signal is modeled as

$$y(n) = [h(n) \otimes x(n) + \omega(n)]e^{j2\pi\varepsilon n/N} \quad (31)$$

ε is the relative carrier frequency offset normalized by the subcarriers frequency spacing). The received data are filtered by a narrow band filter with pass band being the bandwidth of synchronization signals, i.e., 1.08 MHz, so that the non-PSS subcarriers are filtered out. Without the interference of non-PSS subcarriers, received PSS data in time domain reserves symmetric property, Then the data are down sampled to 1.92 MHz with FFT size N = 128. With this low sampling rate at receiver, the symbol duration is enlarged so that the influence of multipath delay is minimized.

As mentioned in the last section, the cross correlation between received PSS and local PSS in time domain can be written as

$$R_u(d) = \left| \sum_{n=0}^{N-1} y(d+n).(P_{time}^{(u)}(n))^* \right|^2 \quad (32)$$

In order to reduce the impact of frequency offset, M-part correlation was proposed in [19]. The received PSS and local PSS in time domain are divided into M segments, symbol timing can be obtained by the cross correlation of corresponding segment. The timing metric is described as follows

$$R_u(d) = \sum_{m=0}^{M-1} \sum_{n=0}^{\frac{128}{M}-1} \left| y\left(d+n+\frac{128.m}{M}\right).(P_{time}^{(u)}(n+\frac{128.m}{M}))^* \right|^2 \quad (33)$$

Where M denotes the segments, 128/M is the length of correlation. According to [16], the performance of anti frequency offset is improved by Partial correlation timing synchronization algorithm, but with the increasing of the number of M, performance of synchronization under same SNR will lose, the selection of M need to compromise. Empirical value of M is 4.

4.3.2. Symbol Timing Synchronization Based on Partial Correlation Timing Synchronization Algorithm.

In order to improve the performance of synchronization and eliminate the defect of M-part correlation algorithm, a novel method has been proposed which rely on partial correlation timing synchronization algorithm.

The received PSS and local PSS in time domain are divided into four segments, Correlation result is shown as follows.

$$A(d) = \sum_{n=0}^{32-1} y(d+n+32.m).(P_{time}^{(u)}(n+32.m))^* \quad (34)$$

Symbol timing can be obtained by the differential correlation of four segments' cross correlation.

$$R_u(d) = \sum_{m=0}^{2} A_m(d)A_{m+1}(d)^* \quad (35)$$

According to [18] It's proved that the correlation of A with sum of B and C equals to the sum of correlations of A with B and A with C.

Therefore, the sum of correlations of three separate PSS sequences equals to the correlation of the sum of PSS sequences.

$$P_{time}(n)=P_{time}^{25}(n)+P_{time}^{29}(n)+P_{time}^{34}(n) \quad (36)$$

A correlation between the received samples and the sum of local PSS sequences can be performed. Using only one correlation, the UE can get a sharp peak to establish the symbol timing synchronization position.

At the same time, in order to further improve the performance of timing detection under large frequency offset, and eliminate burst and random of the estimation results, the author took cumulative processing of the received data. Data accumulation process is shown as in Figure 4.1.

$$A(d) = \sum_{n=0}^{32-1} y(d+n+32.m).\left(P_{time}(n+32.m)\right)^* \quad (37)$$

$$R_u(d) = \frac{1}{K}\sum_{m=0}^{K-1}\sum_{m=0}^{2} A_m(d)A_{m+1}(d)^* \quad (38)$$

Where K is the accumulation number of half frame

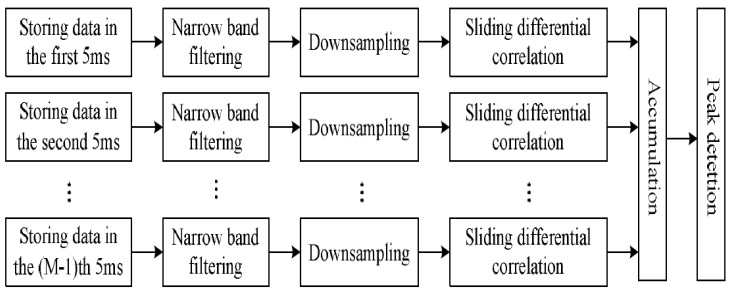

Figure 4.1 Data Accumulation process

4.4. Low Complexity Cell Search Scheme Using GAUSSIAN INTEGER PERFECT SEQUENCE (GIPS) [20].

In [20] the authors presented a new technique based on (GIPS) of length 16N to represent the primary and secondary synchronization sequences.

But in this method, the authors focused on proposing the new technique to get $\mathrm{N}_{\mathrm{ID}}^{(1)}$.

Two groups of base sequences is proposed, each having four base sequences. The length N of each base sequence is a multiple of 16. A perfect sequence can be obtained by linearly combining these eight base sequences or their cyclic shift equivalents with nonzero complex coefficients of equal magnitude. These two groups of base sequences are denoted by $x_i[n]$ and $y_i[n]$, respectively, $i = 1, 2, 3, 4$, $n = 0, 1, \ldots, N-1$. The first group of base sequences can be written as four vectors:

$$\mathbf{x}_1 = [1, \underbrace{0 \cdots, 0}_{\frac{N}{4}-1}, 1, \underbrace{0 \cdots, 0}_{\frac{N}{4}-1}, 1, \underbrace{0 \cdots, 0}_{\frac{N}{4}-1}, 1, \underbrace{0 \cdots, 0}_{\frac{N}{4}-1}],$$

$$\mathbf{x}_2 = [1, \underbrace{0 \cdots, 0}_{\frac{N}{4}-1}, j, \underbrace{0 \cdots, 0}_{\frac{N}{4}-1}, -1, \underbrace{0 \cdots, 0}_{\frac{N}{4}-1}, -j, \underbrace{0 \cdots, 0}_{\frac{N}{4}-1}],$$

$$\mathbf{x}_3 = [1, \underbrace{0 \cdots, 0}_{\frac{N}{4}-1}, -1, \underbrace{0 \cdots, 0}_{\frac{N}{4}-1}, 1, \underbrace{0 \cdots, 0}_{\frac{N}{4}-1}, -1, \underbrace{0 \cdots, 0}_{\frac{N}{4}-1}],$$

$$\mathbf{x}_4 = [1, \underbrace{0 \cdots, 0}_{\frac{N}{4}-1}, -j, \underbrace{0 \cdots, 0}_{\frac{N}{4}-1}, -1, \underbrace{0 \cdots, 0}_{\frac{N}{4}-1}, j, \underbrace{0 \cdots, 0}_{\frac{N}{4}-1}].$$

The nth element of each of the four base sequences can be represented as:

$$x_i[n] = e^{j\frac{2\pi(i-1)n}{N}} . \delta\left[n - \left\lfloor \frac{4n}{N} \right\rfloor . \frac{N}{4}\right] \tag{39}$$

where $i = 1, 2, 3, 4$, $n = 0, 1, \ldots, N-1$.

The second group of base sequences can also be written as four vectors:

$$\mathbf{y}_1 = [1,\ 1,\ 1,\ 1,\ 1,\ 1,\ 1,\ 1, \ldots,\ 1,\ 1,\ 1,\ 1]_{1\times N},$$
$$\mathbf{y}_2 = [1, j, -1, -j, 1, j, -1, -j, \ldots, 1, j, -1, -j]_{1\times N},$$
$$\mathbf{y}_3 = [1, -1, 1, -1, 1, -1, 1, -1, \ldots, 1, -1, 1, -1]_{1\times N},$$
$$\mathbf{y}_4 = [1, -j, -1, j, 1, -j, -1, j, \ldots, 1, -j, -1, j]_{1\times N}.$$

The *n*th element of each of the four base sequences has the following form:

$$y_i[n] = e^{j\frac{\pi(i-1)n}{2}} \tag{40}$$

The Gaussian integer perfect sequence is

$$\mathrm{z[n]} = \sum_{\mathrm{i=1}}^{4}\{\frac{\mathrm{N}}{4}.\mathrm{c_i}.\mathrm{x_i}[(\mathrm{n}-\mathrm{s_i})_\mathrm{N}] + (\mathrm{b_i}-\mathrm{c_1}).\mathrm{y_i}[(\mathrm{n}-\mathrm{s_1})_\mathrm{N}]\} \tag{41}$$

Finally according to [20], the discrete Fourier transform (DFT) of the GIPS is written as following

$$Z[m] = \sum_{i=1}^{4}\left\{\frac{N}{4}.c_i.e^{-j\frac{2\pi s_i m}{N}}.X_i[m] + (b_i - c_1).e^{-j\frac{2\pi s_1 m}{N}}.Y_i[m]\right\} \tag{42}$$

Where $m = 0, 1, \ldots, N-1$, $X_i[m]$ and $Y_i[m]$ are the DFT of $x_i[n]$ and $y_i[n]$, respectively, and written as

$$X_i[m] = 4.\delta[m - \left\lfloor\frac{m}{4}\right\rfloor.4 - (i-1) \tag{43}$$

$$Y[m] = 4.\delta[m - \frac{N}{4}.(i-1)] \tag{44}$$

$b_i$and c_i, are arbitrary nonzero Gaussian integer numbers of equal magnitude,

and $s_i \in \{0, 1, \ldots, N-1\}$, $i = 1, 2, 3, 4$.

In [20] a low-complexity scheme is proposed to obtain the Cell-ID.

The primary synchronization signal presented in chapter 3 is re-written as

$$P_p[n]\begin{cases} Z_p[n] & n = 0, 1, \ldots, 31 \\ 0 & n = 32 \\ Z_p[n-32] & n = 33, 34, \ldots, 63 \end{cases} \tag{45}$$

Where $p = 0, 1, 2$ represents the type of the primary synchronization signal

$$Z_p[m] = \sum_{i=1}^{4}\left\{\frac{N}{4}.c_i.e^{-j\frac{2\pi s_i m}{N_s}}.X_i[m]\right\} \tag{46}$$

$N_s = 32$, c = $[c_1\ c_2\ c_3\ c_4]$ are the same for all three primary synchronization signals, c = [1 − 1 − 1 − 1], and $\mathrm{s_i}$ are [0 1 2 3],[0 2 4 6],[0 3 6 9], respectively, for three different types primary synchronization signals.

The secondary synchronization signals are represented as follows

$$S_{q,r}[n]\begin{cases} Z_q[n] & n = 0, 1, \ldots, 31 \\ 0 & n = 32 \\ Z_q[n-32] & n = 33, 34, \ldots, 63 \end{cases} \tag{47}$$

Where q represents $\mathrm{N_{ID}^{(1)}}$ index and r = 1, 2.

$$Z_q[m] = \sum_{i=1}^{4} \left\{ \frac{N}{4} . c_{r,i} . e^{-j\frac{2\pi s_i m}{N_s}} . X_i[m] \right\} \quad (48)$$

$c_r = [c_{r,1}\ c_{r,2}\ c_{r,3}\ c_{r,4}] = e^{j(r-1)}.[1 -1 -1 -1]$ and $s_{q,1} = 0$, and $s_{q,2}$, $s_{q,3}$ and $s_{q,4}$ are arbitrary integer values between 0 to 3 but $s_q = [s_{q,1}\ s_{q,2}\ s_{q,3}\ s_{q,4}] \notin$ {[0 1 2 3], [0 2 4 6], [0 3 6 9]}.

The cell search is performed as follows.

Since the traditional cell-ID group acquisition scheme requires high computational complexity. cell-ID acquisition scheme is presented here and the other parts of the cell search procedure are the same as the traditional scheme, e.g. the method to obtain $N_{ID}^{(2)}$ is the same as the traditional scheme by computing the correlation between the received signal and all transmitted sequences. The received P-SCH and S-SCH signals are written as following, respectively

$$R_{PSCH}[n] = H_p[n].P_p[n] + W_p[n] \quad (49)$$

$$R_{SSCH,r}[n] = H_r[n].S_{q,r}[n] + W_r[n] \quad (50)$$

Where r = 1, 2, $H_p[n]$ and $H_r[n]$ are the channel response, and $W_p[n]$ and $W_r[n]$ are the additive white Gaussian noise.

According to [20] we can get $N_{ID}^{(1)}$ as follows

The r[th] received S-SCH signal, $R_{SSCH,r}[n]$, firstly multiplies by the conjugate of the closely received P-SCH signal, $R_{PSCH}[n]$, as following

$$M_r[n] = R_{SSCH,r}[n].R_{PSCH}[n]^* = \{H_r[n].S_{q,r}[n] + W_r[n]\}.\{H_p[n].P_p[n] + W_p[n]\}^* \quad (51)$$

$$= \frac{N^2}{16} . e^{j(r-1)} . e^{j\frac{8\pi(s_{p,t}-s_{q,t})n}{N} + W''[n]}$$

Where $W''[n] = H_r[n].S_{q,r}[n].W_p^*[n] + H_p^*[n].P_p^*[n].W_s[n] + W_s[n].W_p^*[n]$

After obtaining $s_{q,t}$, the corresponding index of s_q means the index of cell-ID groups, i.e. $N_{ID}^{(1)}$.

4.5. Frequency Domain Based Method for Symbol Timing Estimation

As shown in the previous researches, the computational complexity of the received synchronization system is a very important point considered in the system efficiency. Since the computational capability of a UE is much lower than that of an eNB, a low-complexity PSS detection algorithm is critical to simplify the UE's operation when it is in a high-speed mobility environment and very frequently perform the handover [1].

In [17], the AHC detector achieves half of the complexity with the same performance of the conventional detector where the receiver performs cross correlation between three replicas of the PSS and received PSS in time domain. The authors also defined that the CSC detector achieves 0.25 of the conventional detector complexity but however, with a cost of a slight accurate degradation. The authors stated that both detectors are very sensitive to the frequency offset. According to [18] the partial correlation method is almost the same complexity of the conventional time domain method with better performance in larger frequency offset when M = 4 in equation (33). The new method the authors introduced in [18] achieves almost the half complexity of the conventional one when K= 3 in equation (38). In [20] the authors only used the GIPS to get $N_{ID}^{(1)}$ and they estimate $N_{ID}^{(2)}$ using the conventional detector.

We can conclude from the previous researches that more efforts should be made to simplify the synchronization receiver complexity and eliminate the frequency offset as well. This will help us to improve the system latency to achieve the high capabilities of the LTE specifications.

In our thesis a new technique is proposed in frequency domain to get the primary synchronization sequence start which is used to determine the sub-frame start (with uncertainty if it is sub-frame 0 or sub-frame 5) and then use the secondary synchronization sequence as shown in [4] to get the sub-frame number.
In our new technique, we use the cyclic prefix based method to get the fractional part of the frequency offset only, as shown above. We use the Frequency domain based method to get the symbol timing start as will be shown.

This novel method will help us to achieve lower complexity with more than one hundred times the conventional time domain method, which will achieve a great effect in simplifying the applied receiver in the industrial applications of the LTE systems.

It is shown in [1] that the primary synchronization sequence is mapped on the 62 mid sub-carriers located around the DC-carrier in frequency domain, so in this method we make a window with the FFT length (N) and apply FFT with this length on N received samples from the received frame as shown in (52).
After the FFT operation we extract the 62 mid sub-carriers located around the DC-carrier which may contain the primary synchronization sequence. We repeat this step for the next N received samples with window step M, where $M=2^x$ x=0,1,……ln(N) as shown in figure 4.2.

$$Y(k) = \sum_{n=0}^{N-1} y_1(n) e^{-i2\pi k \frac{n}{N}} \quad k = 0, \dots\dots\dots, N-1 \tag{52}$$

Now we perform a cross correlation of $Y'(k)$ (the FFT output after extracting the 62 mid sub-carriers located around the DC-carrier) with replicas of the three primary synchronization signals in the frequency domain as shown in (53) and repeat this process for a half frame.

$$R_i(l) = \sum_{k=-31, k\neq 0}^{31} d_i^*(k).Y'(k+l) \tag{53}$$

where $d_i(n)$ is the primary synchronization signal (i=25, 29, 34).
We choose the FFT output, where the magnitude of the correlation output $|R_i(l)|$ shows a large peak compared to the other sequences, so this window with length N includes the primary synchronization sequence. Also we know the root index of the transmitted primary synchronization signal, so we can know $N_{ID}^{(2)}$ as shown in (1) and table 3.1.

Now we want to estimate the accurate position of the primary synchronization signal in this window, so we set all the sub carriers data to zero in the frequency domain, except the 62 mid sub-carriers located around the DC-carrier which contain the primary synchronization signal, then perform IFFT for the 62 mid sub-carriers with length N, so we have these subcarriers now in time domain.

We perform a cross correlation for the IFFT output with the primary synchronization signal with the root index estimated in (53) in the time domain as shown in (54). The output of the cross correlation shows a large peak at the start of the primary synchronization sequence in this window.

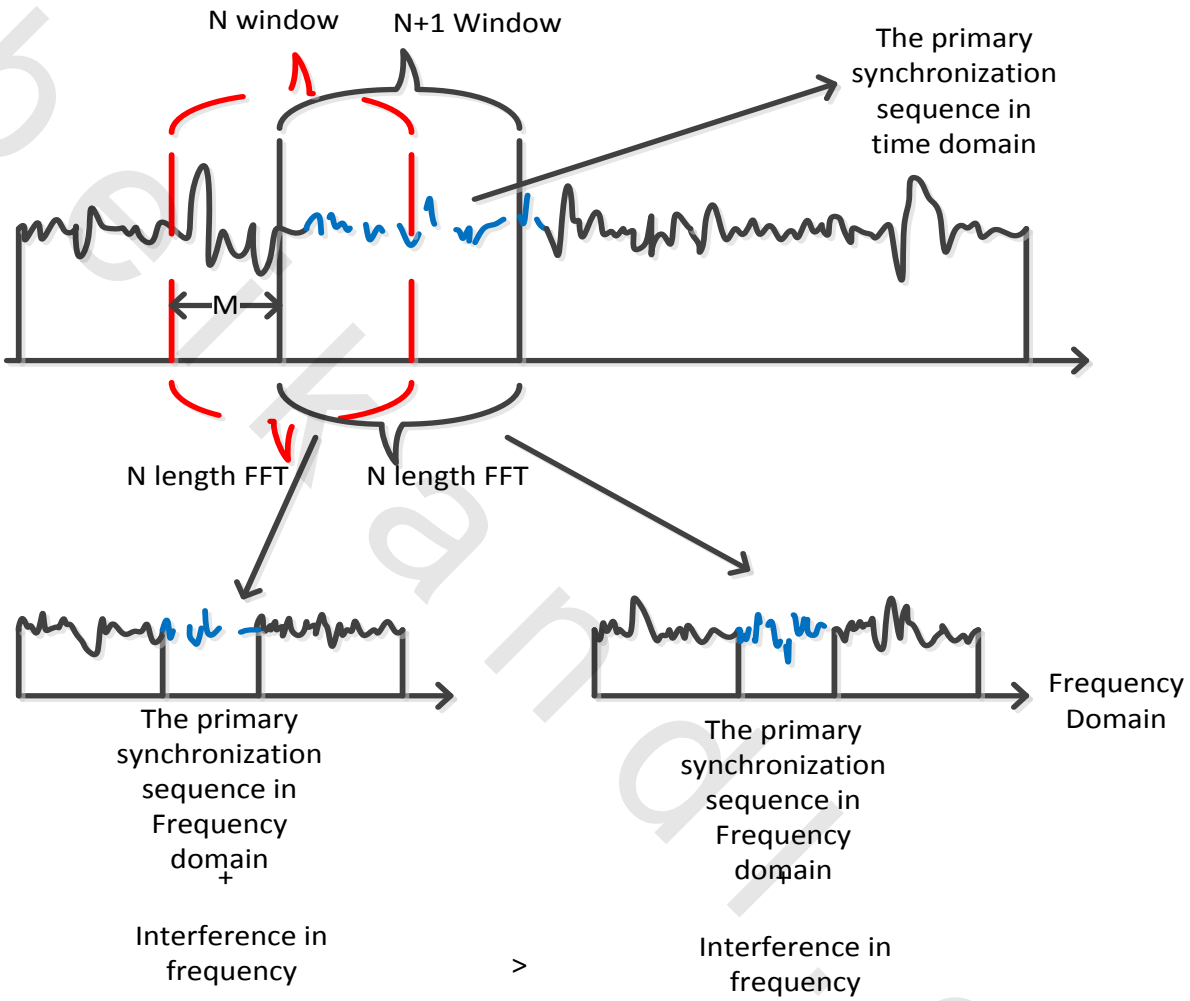

Figure 4.2 The received OFDM symbols in time and frequency domain with window step size = M in Frequency Domain based method.

$$R(l) = \sum_{n=-N/2, n\neq 0}^{N/2} d^{*}_{|R(l)|_{max}}(n).y''(n+l) \qquad (54)$$

Where $d_{|R(l)|_{max}}(n)$ is the primary synchronization signal with the root index estimated in (53) in time domain and $y''(n)$ is the 62 mid sub-carriers located around the DC- carrier in time domain.

We can improve the performance of Frequency domain based method by applying it for the second half of the frame, as the primary synchronization sequence is mapped to the last OFDM symbol in slot 0 and slot 10 (in sub-frame 0 and 5) in time domain [1] and averaging the output of the first and second half frame.

We can see here in the Frequency domain based method that extracting the 62 mid sub-carriers located around the DC-carrier is performed in the frequency domain, so no side lobes or residual frequencies are found, and we can get the mid sub-carriers accurately.
If we make the filtration process in time domain, no ideal filter is available in time domain, we will suffer from noise effects in the output and we will make additional computations to get the 62 mid sub-carriers located around the DC-carrier using the filter.

Another advantage in our method is that the complexity is less than the conventional method. In the conventional method, which we will compare our proposed method with it in the next chapter, we are correlating N symbols from the received frame with replicas of the three primary synchronization signals in time domain and repeating this step every N symbols with window step equals one. We repeat the correlation process for half frame. If we did not detect a primary sequence, we repeat these steps for the next half frames, till we detect a PSS and estimate $N_{ID}^{(2)}$. In our method the window step equals M so the number of the multiplications and additions are decreased.

The Frequency domain based method is homogenous with the conventional system after the synchronization as we perform FFT on the received symbols to complete the receiver process.

Note: In case of M = N = full FFT length, We combine every two consecutive FFT outputs with each other as shown in (55), (56) and (57) to guarantee the presence of the whole primary sequence if we extracted part of them in one window as shown in Figure 4.3.

$$Y_1(k) = \sum_{n=0}^{N-1} y_1(n) e^{-i2\pi k \frac{n}{N}} \quad k = 0, \dots\dots\dots, N-1 \tag{55}$$

$$Y_2(k) = \sum_{n=0}^{N-1} y_2(n) e^{-i2\pi k \frac{n}{N}} \quad = 0, \dots\dots\dots, N-1 \tag{56}$$

$$Y'(k) = Y'_1(k) + Y'_2(k) \quad (57)$$

We continue as mentioned above and after the cross correlation process, we choose the two consecutive FFT outputs, so this window with length 2N includes the primary synchronization sequence.

To estimate the accurate position of the primary synchronization signal in this window, we set all the sub-carriers to zero in the frequency domain, except the 62 mid sub-carriers located around the DC-carrier in both FFT outputs, perform IFFT for the 62 mid sub-carriers with length N for every FFT output and continue as mentioned above.

We can see in Figure 4.4 the flow chart of the proposed frequency domain based method.

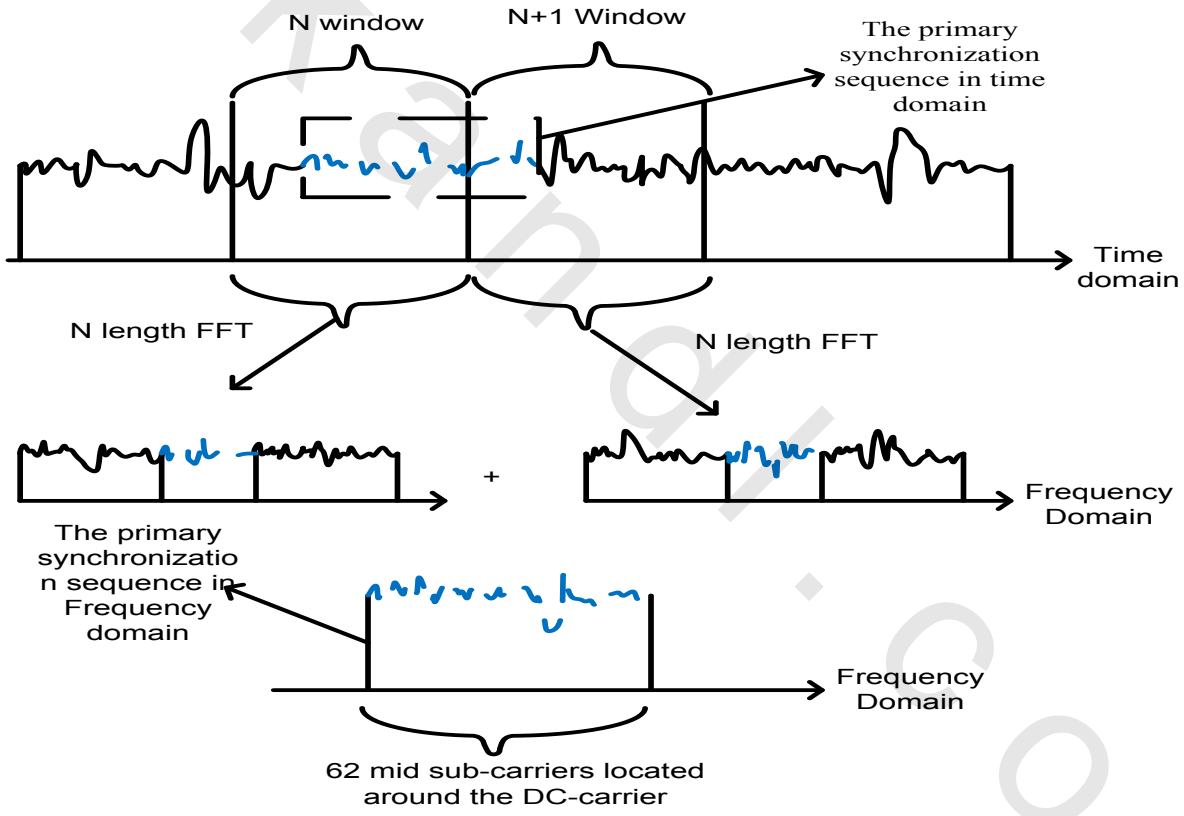

Figure 4.3 The received OFDM symbols in time and frequency domain in case of the presence of the primary sequence in two OFDM symbols with M=N.

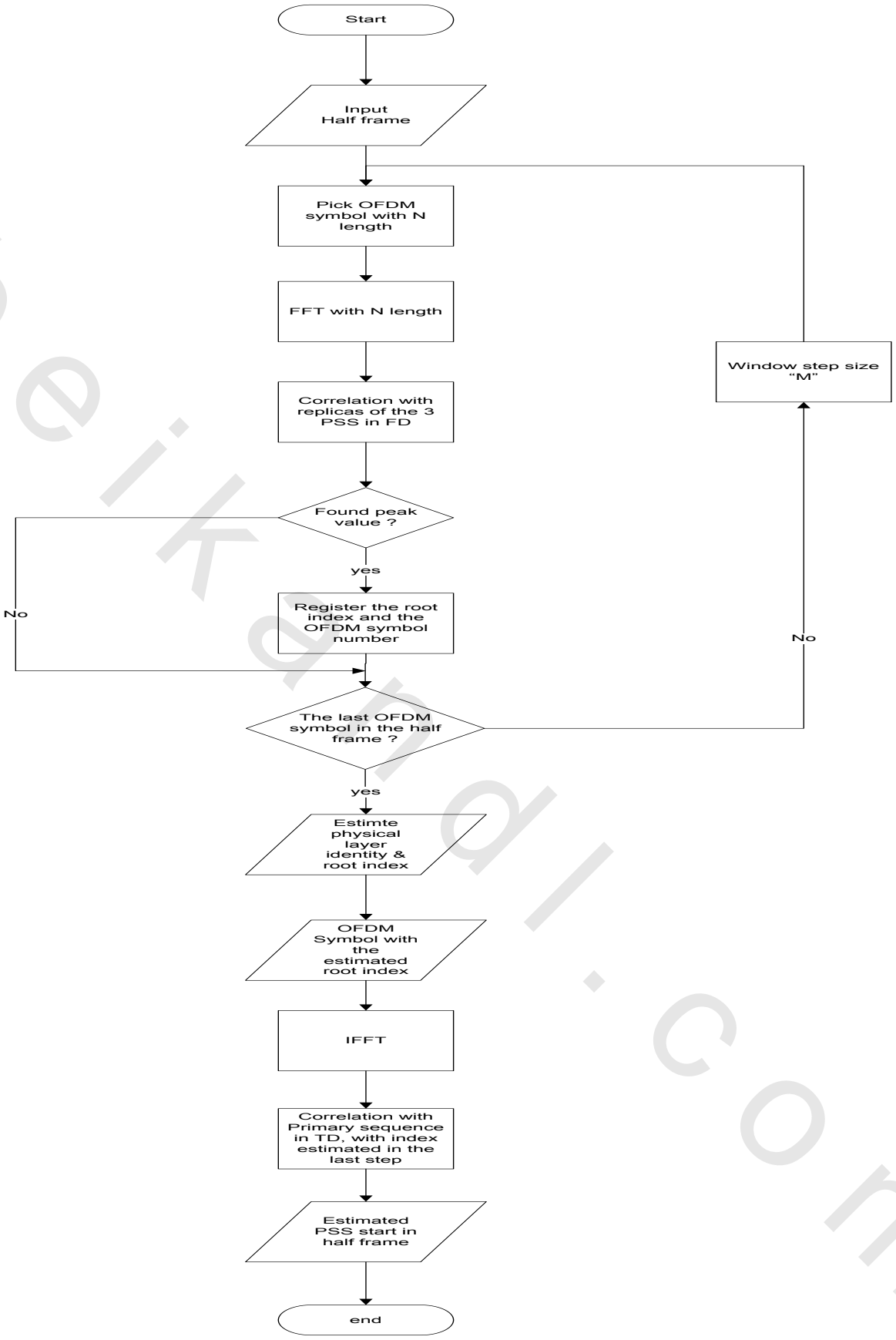

Figure 4.4 Flow chart of the frequency domain based method

4.6. Group and Cell Search

The cell-ID needs to be estimated correctly, in order to establish connection with the best possible serving base station.

At the same time, the cell-ID is required for extracting the reference sequence entries from proper sub-carrier positions, and perform afterwards a channel estimation via interpolation in frequency domain.

The group-ID Ng can be jointly estimated with the sub-frame index within the radio frame (0 or 5).

The basic concept is to exploit the cyclic shifts of the two length-31 binary sequences $s_0(n)$ and $s_1(n)$ according to the pair of integers m_0 and m_1, which identify the group-ID.

First, we extract the 62 mid sub-carriers of the OFDM symbol of the secondary synchronization signal to get $d(n)$ in frequency domain and separate it into odd and even pairs.

Then, We get the sequence $s_0^{(m_0)}$ and exploit the cyclic shifts of it using cross correlation calculations to estimate m_0 .

After that, we can get $s_1^{(m_1)}$ and m_1 respectively with the same method.

Finally we can estimate the sub-frame index using cross correlation between the extracted secondary synchronization signal and the estimated secondary synchronization signals in sub-frame 0 and sub-frame 5 which are estimated using m_0 and m_1, as shown in (58) and (59).

$$d_{est}(2n) = \begin{cases} s_0^{(m_{0est})}(n)c_0(n) & \text{in subframe 0} \\ s_1^{(m_{1est})}(n)c_0(n) & \text{in subframe 5} \end{cases} \quad (58)$$

$$d_{est}(2n+1) = \begin{cases} s_1^{(m_{1est})}(n)c_1(n)z_1^{(m_{0est})}(n) & \text{in subframe 0} \\ s_0^{(m_{0est})}(n)c_1(n)z_1^{(m_{1est})}(n) & \text{in subframe 5} \end{cases} \quad (59)$$

The magnitude of the correlation output shows a large peak with the estimated sub-frame index as shown in (58).

$$R_i(l) = \sum_{k=-31, k\neq 0}^{31} d_i^*(k).\, d_{est}(k+l) \quad (58)$$

Where (i=0,5) and $d_i^*(n)$ is the extracted secondary synchronization signal.

The pair of estimated m0 and m1 identifies the group-ID $N_{ID}^{(2)}$ so we can compute the overall cell-ID: $N_{ID}^{cell} = 3N_{ID}^{(1)} + N_{ID}^{(2)}$.

The block diagram in figure 4.5 summarizes the frequency domain based method.

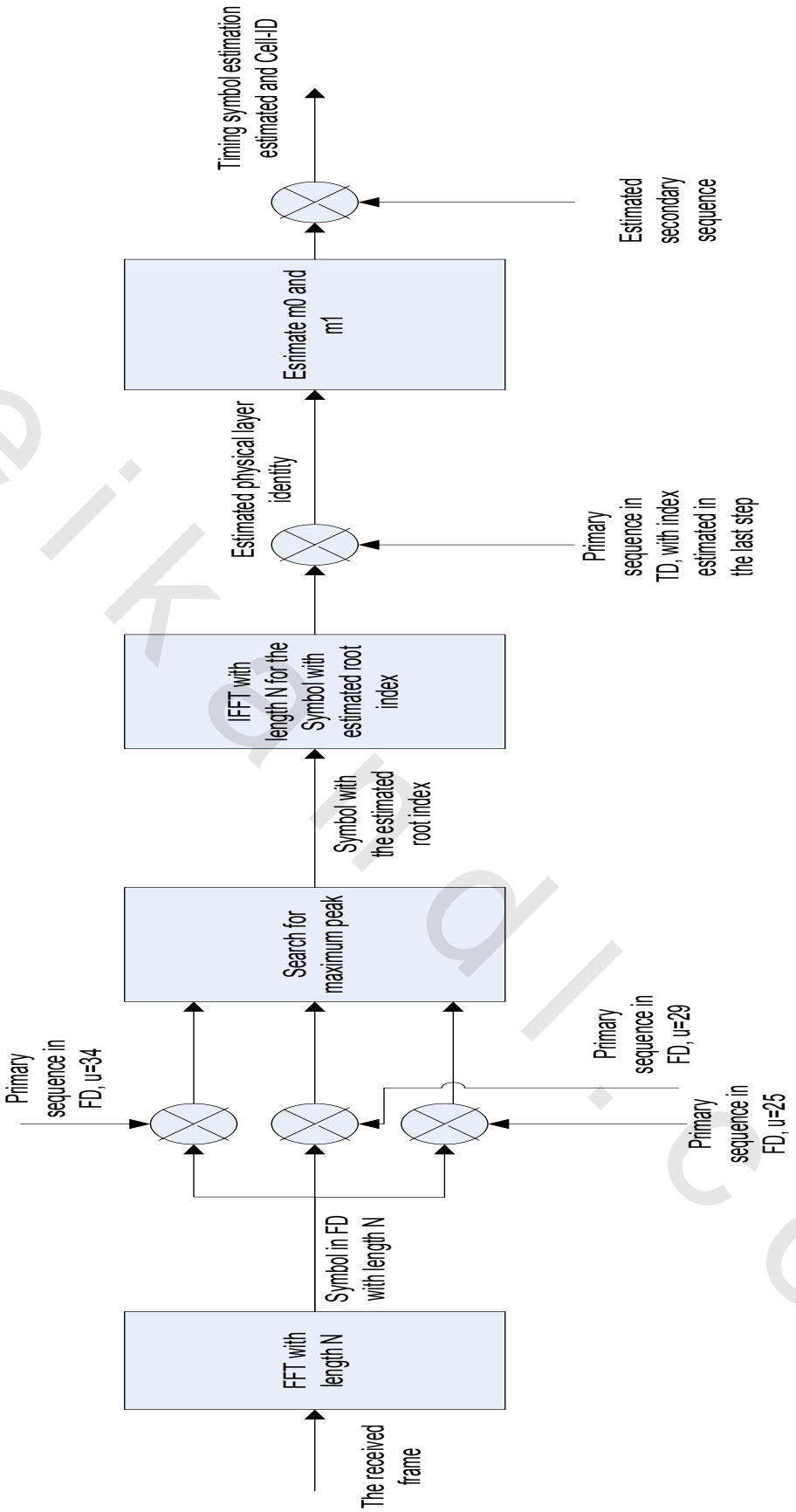

Figure 4.5 Block diagram of the frequency domain based method